

## Application of non-biological surrogates for analysis of sequential disinfection continuous flow systems

Brannon Richards and Joel Ducoste

### ABSTRACT

Fluorescent YG-microspheres (Polysciences Inc.) were evaluated to simulate *Cryptosporidium* inactivation in a continuous flow system that utilizes multiple disinfectants. Experiments were performed in a disinfection process consisting of an ozone primary stage and a secondary free chlorine stage. Impacts of the chemical disinfectant exposure were calculated by tracking the changes in fluorescence distribution with a flow cytometer. Tests were performed at two flow rates (11- and 15.5-ml/s) and a target concentration-time (Ct) product of 1.4 mg/L-min for ozone and 510 mg/L-min for chlorine. Analysis of the results suggest that the fluorescence decay of YG-fluorescent microspheres does display synergistic effects when free chlorine is used sequentially with ozone in a continuous flow system. The study also included the use of a simple Segregated Flow Reactor (SFR) model to simulate the sequential disinfection process. The model was not effective at predicting fluorescent intensity changes at different intermediate points within the disinfection process stream due to the complexity of the paths taken by the microspheres through the ozone primary disinfectant chamber and its eventual influence on chlorine secondary disinfectant kinetics. An ozone Ct distribution, which utilized the fluorescence microspheres experimental data and was created from the range of paths traveled by the microspheres, displayed a range of Ct values between 0.5 to 3.2 mg/L-min for the low flow condition and 0.8 to 2.2 mg/l-min for the high flow condition. A new model structure was proposed that may improve the simulation of sequential disinfection systems.

**Key words** | chlorine, Ct distribution, fluorescence microspheres, ozone, sequential disinfection, water treatment

**Brannon Richards**  
**Joel Ducoste** (corresponding author)  
Department of Civil, Construction, and  
Environmental Engineering,  
North Carolina State University,  
208 Mann Hall CB 7908,  
Raleigh, NC 27695-7908,  
USA  
E-mail: [jducoste@eos.ncsu.edu](mailto:jducoste@eos.ncsu.edu)

### INTRODUCTION

The primary goal of disinfection in drinking water treatment is to inactivate microorganisms capable of causing waterborne disease outbreaks. This task has become more challenging with the existence of resistant pathogenic organisms such as *Cryptosporidium*. Due to the dangers associated with *Cryptosporidium*, the EPA has developed rules to limit human exposure through drinking water (US Environmental Protection Agency 1998, 2002). These stricter regulations have forced researchers to focus on the removal of *Cryptosporidium*.

Studies have shown that the use of free or combined chlorine, the most widely used disinfectants, have little or

no effect alone on *Cryptosporidium* due to its resistant outer shell (Gyurek *et al.* 1997; Driedger *et al.* 2000). The ability of *Cryptosporidium* to form this resistant outer shell has led researchers to investigate the use of other chemical disinfectants such as ozone and chlorine dioxide. However, the concern that high concentrations of ozone or chlorine dioxide can lead to the formation of carcinogenic disinfection by-products has resulted in researchers looking for new approaches to reduce their usage (Liyanage *et al.* 1997; Driedger *et al.* 2000; Rennecker *et al.* 2000b, 2001; Li *et al.* 2001a; Baeza & Ducoste 2004).

doi: 10.2166/aqua.2008.042

These approaches call for two disinfectants used sequentially to inactivate *Cryptosporidium* (Liyana *et al.* 1997; Rennecker *et al.* 2000a,b, 2001; Li *et al.* 2001a,b; Corona-Vasquez *et al.* 2002a,b). Li *et al.* (2001a) have shown that sequential inactivation using ozone followed by free or combined chlorine increased the inactivation of *Cryptosporidium* compared to the individual use of these disinfectants. Driedger *et al.* (2000) showed that ozone and free chlorine used sequentially led to a substantially higher *Cryptosporidium* inactivation rate constant for free chlorine than when chlorine was used alone. This synergistic mechanism has been explained by improved chlorine permeation through *Cryptosporidium*'s cell wall due to damage caused by the initial ozone exposure (Driedger *et al.* 2000).

To date, most *Cryptosporidium* inactivation studies have been done at the bench scale. The problem with designing full-scale reactors is that the Cts (disinfectant concentration  $\times$  exposure time, based on time that 10% of influent water reaches the effluent) from batch reactors do not completely describe the system hydraulics since it is only one point in the residence time distribution (RTD). If the system was over-designed, then high disinfectant concentrations would result in excessive treatment cost and greater formation of disinfection by-products. However, reactor under-design could lead to *Cryptosporidium* breakthrough into the drinking water distribution system (Mariñas *et al.* 1999). As a result, direct quantification of disinfection performance is preferred to better evaluate *Cryptosporidium* inactivation. Alternatives include development of more accurate Ct values by continuously monitoring disinfectant concentration distribution and hydraulics mixing throughout the reactor. This can be accomplished by performing chemical tracer tests for hydraulic characterization and using inactivation models to simulate organism disinfection behavior (Vasconcelos *et al.* 1997; Haas *et al.* 1998). Other alternatives include the use of biological (Kim *et al.* 2002) and non-biological (Chiou *et al.* 1997; Mariñas *et al.* 1997, 1999; Baeza & Ducoste 2004) surrogate indicators.

Non-biological indicators are of particular interest, since no special biological facilities are needed. Direct quantification can be made with the surrogate, since it already takes into account system hydraulics. The non-biological surrogate

indicators, which have been used for chemical disinfection performance, are fluorescent dye polystyrene microspheres. These non-biological microspheres have been used by Chiou *et al.* (1997) to mimic *Giardia* inactivation with ozone disinfection, by Mariñas *et al.* (1999) to mimic *Cryptosporidium* inactivation with ozone disinfection in batch and full-scale water treatment plants, and recently by Baeza & Ducoste (2004) to mimic *Cryptosporidium* sequential disinfection in batch reactors. All of these studies have shown promising results in using microspheres to mimic microbial inactivation. However, no study has used microspheres with sequential disinfection in a continuous flow system to mimic *Cryptosporidium* inactivation. Hence, this study was performed to evaluate this non-biological approach in continuous-flow sequential disinfection processes.

## EXPERIMENTAL MATERIALS AND METHODS

### Description of microspheres

The non-biological surrogates used were YG Fluoresbrite™ fluorescent microspheres with a diameter of 0.94  $\mu\text{m}$  (2% coefficient of variation) and a density of 1.045  $\text{g}/\text{cm}^3$ . The commercial microspheres from Polysciences Inc. come stored in an aqueous solution with 2.6% solids content. Preliminary tests showed that the original microspheres contained more fluorescent dye than required to simulate the inactivation of *Cryptosporidium*. Thus, the microspheres were pretreated with ozone to lower their fluorescence (Mariñas *et al.* 1997; Baeza & Ducoste 2004). The pretreatment step will be explained in a subsequent section. The dye had an unknown chemical formula created by Polysciences Inc. However, a previous study showed that the fluorescence of the YG fluoresbrite matches the fluorescence characteristics of fluorescein isothiocyanate (Mariñas *et al.* 1997).

### Experimental apparatus

The continuous-flow sequential disinfection system consisted of four bench scale reactors in series: two initial ozone contactors followed by a chlorine-mixing chamber

and finally, a chlorine baffled contactor. Influent tap water that contained free and combined chlorine was filtered and deionized by a Bantam Deionizer (activated carbon followed by two 2-bed ion exchange cartridges, Models 8904 and 8901; Barnstead International, Dubuque, IA) to remove these compounds as well as other organic compounds that react with ozone and chlorine. The influent water was pumped to the 1st ozone contactor. Tests were performed with the source water to make sure that the free and combined chlorine concentrations were zero. However, some ammonium from the destruction of the combined chlorine species may have been released into the pilot-scale system. Thus, additional combined chlorine measurements were performed within the pilot system following free chlorine addition and will be discussed in a subsequent section. The pretreated microspheres were injected 35 pipe diameters upstream from the initial two ozone bubble column contactors with an influent peristaltic pump to completely mix the microspheres solution with the main flow stream. The experiments were performed at two influent flow rates, 11.0- and 15.5-ml/s, that was the maximum flow for the pilot system. The flow of the water/microsphere mixture is shown in Figure 1.

The ozone contactors were 60 cm tall with a diameter of 7.5 cm. A stone diffuser that covered a large portion of the ozone contactor bottom was used to inject the ozone gas. The water/microsphere mixture flowed cocurrent with the ozone in the first contactor and countercurrent

to the ozone in the second contactor. A Model G-11 Ozone-Pacific corona discharge generator was used to produce ozone with dried industrial air at a flow rate of 10 SCFH (standard cubic feet per hour). The ozone concentration was controlled with a variable control knob that operates from 0 to 100% of the ozone output. All experiments were performed at room temperature ( $20 \pm 2^\circ\text{C}$ ).

A 12 cm diameter mixing chamber was used to blend chlorine with the water/microsphere mixture after ozone treatment. Chlorine was injected with a peristaltic pump into the  $1000\text{ cm}^3$  mixing chamber at a rate of 0.255 ml/s. The effluent water was pumped by a second peristaltic pump into the chlorine contactor that had an overall width of 61 cm and an overall length of 37.5 cm. The water height within the contactor was maintained at 13.5 cm. The contactor had three baffles that split the contactor into four equal sections of 61 cm by 9 cm. An additional three baffles, oriented vertically from the free surface to a height 2 cm above the contactor bottom, were used to promote additional top to bottom mixing. Figure 1 displays the baffles located within the chlorine contactor as well as the water/microsphere flow pattern.

### Ozone disinfection

In this research, ozone was applied to the microspheres to perform two tasks. Ozone was first used to pretreat the

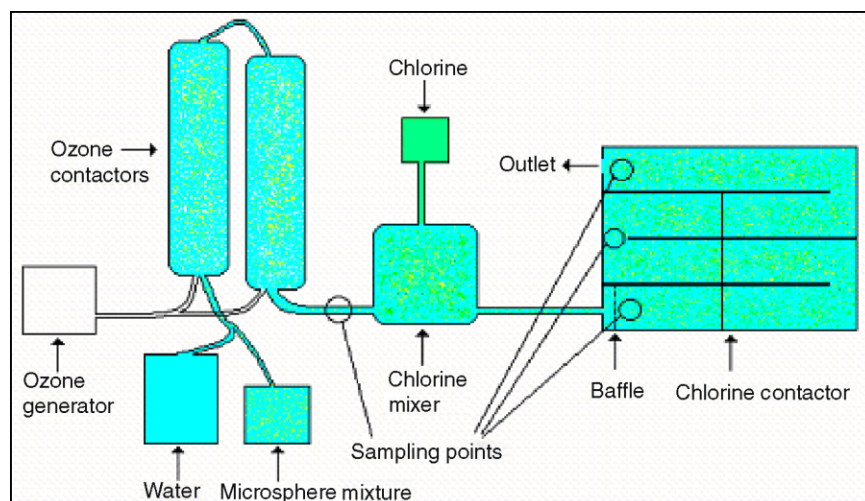


Figure 1 | Sequential disinfection of continuous-flow system.

microspheres so that the fluorescent decay would closely imitate the inactivation kinetics of *Cryptosporidium* (Baeza & Ducoste 2004). Ozone was later used to act as the primary disinfectant in the continuous flow disinfection process.

### Microsphere pretreatment

In the pretreatment step, one litre of 0.01 M phosphate buffer at pH 7.5 was placed in a semi-batch reactor where ozone was bubbled for at least 20 minutes to ensure a steady state concentration of  $0.30 \pm 0.03$  mg/L. The ozone concentration was measured (50 ml of sample) by an Indigo Pocket Colorimetric Method, Hach Co. (Loveland, Co). After a steady state ozone concentration was reached, approximately  $2.0 \times 10^{10}$  microspheres suspended in 50 ml of pH 7.5 buffer were injected into the batch reactor. The reaction was carried out for a period of 90 minutes. The ozone generator controller knob was then turned to 0% so that only air was bubbled for 20 minutes to remove the residual ozone. The pretreated microspheres were then stored at 4°C.

Following the microsphere pretreatment step, an additional batch test was then performed to determine the fluorescence threshold value, a fitting parameter that allowed the fluorescent microspheres to imitate the *Cryptosporidium* reference data of Driedger *et al.* (2000) as described in Baeza & Ducoste (2004). The batch test was performed much the same as the microsphere pretreatment. Again, ozone gas was bubbled into a semi-batch reactor containing one litre of 0.01 M phosphate buffer at pH 7.5, until a steady state concentration of  $0.30 \pm 0.03$  mg/L was achieved. After a steady state concentration was reached, 50 ml of pretreated microspheres were injected into the system. Samples were taken at time intervals of 30 sec, 60 sec, 2 min, 3 min, 4 min, and 6 min. These sample times were selected such that the microspheres fluorescent intensity decay could be monitored for a Ct of 1.4 mg/L-min (that approximately imitates 1 – log inactivation of *Cryptosporidium*) (Driedger *et al.* 2000). The samples were immediately quenched with 1 ml of 0.1 N sodium thiosulfate to stop all reactions with ozone.

### Primary ozone disinfection

Experiments were performed at ozone concentrations of  $0.35 \pm 0.03$  mg/L in the first reactor and  $0.75 \pm 0.03$  mg/L in the second reactor, to achieve a target 1 – log of microspheres' fluorescence decay for the steady-state flow equal to 15.5 ml/sec. Ozone concentrations within the second ozone contactor were higher because an equal amount of ozone gas was bubbled between the two contactors, and the second contactor received much of the effluent ozone from the first reactor. Low flow experiments (11 ml/sec) were performed with ozone concentrations of  $0.20 \pm 0.03$  mg/L in the first reactor and  $0.38 \pm 0.03$  mg/L in the second reactor to achieve a target 1 – log of fluorescence decay for the microspheres. Experimental measurements of the ozone concentration at different points along the column height were performed to ensure that the target concentration was reached. The ozone concentration was found to be uniform along the column height in both contactors. After steady state was achieved in the reactor, the water/microsphere mixture was continuously injected upstream from the 1st ozone contactor with a microsphere concentration of 70 µg/L. Samples of 50 ml were taken from the effluent of the 2nd ozone contactor to monitor the extent of fluorescence decay prior to injection of chlorine. The ozone in the samples was quenched by adding 4 ml of 0.1N sodium thiosulfate (Fisher Scientific). Due to the low microsphere concentrations, the 50 ml samples were centrifuged at 3,500 rpm for 10 minutes. The concentrated samples were then stored at 4°C and analyzed within 24 hours.

### Sequential disinfection

After contact with ozone, the microspheres flowed by gravity into the chlorine mixing chamber. Ozone concentrations within the chlorine mixing chamber were approximately 0.01 mg/L. The free chlorine secondary disinfection stage was performed at room temperature ( $20 \pm 2^\circ\text{C}$ ). A 1 g/L free chlorine stock solution was prepared with 5% sodium hypochlorite (ACROS Organics). The stock solution was added to the mixing chamber to produce free chlorine concentrations of

approximately  $16.5 \pm 1.0$  mg/L as  $\text{Cl}_2$  during high flow conditions and  $12.4 \pm 1.0$  mg/L as  $\text{Cl}_2$  during low flow conditions. The very high chlorine concentrations were necessitated by the small scale required in the laboratory to obtain the target Ct value. Combined chlorine concentrations were also measured within the reactor system to determine the affect of the released ammonium. Combined chlorine concentrations of approximately  $0.9 \pm 0.1$  mg/L were measured during both low and high flow conditions. Previous experiments have shown that combined chlorine has little effect on the fluorescence decay of the microspheres (Baeza & Ducoste 2004).

The microspheres, already mixed with the free chlorine, were then pumped to the chlorine contactor for further reaction time. Ozone concentrations were measured at several locations within the baffled chlorine contactor. No ozone was found within the contactor. Free chlorine concentrations, within the contactor, were measured by the DPD Pocket Colorimetric Method, Hach Co. (Loveland, Co). Samples of 40 ml were taken from several locations. The free chlorine was immediately and completely reduced to chloride with 4 ml of 0.1 N sodium thiosulfate. A Ct value of 510 mg/L-min was targeted for the chlorine disinfection process to imitate 1 – log of inactivation of *Cryptosporidium* during chlorine sequential disinfection. Measurements of free chlorine in the influent and effluent of the chlorine contactor showed no significant decay in the chlorine concentration and confirmed the target concentration described earlier for each flow rate condition.

Microsphere samples were taken from multiple locations in the flow-through system. The sampling locations are shown in Figure 1. The samples were quenched with 0.1 N sodium thiosulfate in order to remove any remaining ozone or free chlorine within the samples. The flow cytometer used for measuring the microspheres fluorescence was a Becton Dickinson FACSCalibur (Flow cytometer: B.D. Model FACSCalibur, Microbiology and Immunology, College of Veterinary Medicine, NCSU Raleigh NC 27606). At least 10,000 events-microspheres were acquired per sample. The fluorescence intensity results were obtained as histograms that were analyzed by a compatible shareware software called WinMDI Version 2.8 (Windows Multiple Document Interface for Flow

Cytometry) developed by Joe Trotter, Scripps Institute (Trotter 2000). The microspheres survival ratio (N/No) was calculated by selecting a threshold or marker (Mariñas *et al.* 1999; Baeza & Ducoste 2004). The threshold value corresponded to a boundary between the beads representing the viable and non-viable *Cryptosporidium* cysts. A detailed description of the histogram analysis is provided in the literature (Mariñas *et al.* 1999; Baeza & Ducoste 2004).

### Hydraulic characterization

A pulse tracer test was performed to determine the macro-scale mixing characteristics within the different reactors. A known concentration and volume of potassium permanganate dye was injected into the system to perform the pulse tracer tests. Samples of effluent water were taken at small time intervals to capture the shape of the residence time density function (Ducoste *et al.* 2001). The samples were collected and the absorbance measured using a spectrometer to determine the dye concentration at each time interval. Quality assurance was performed on the collected effluent dye concentration that included an assessment of the mass recovered. Only tracer tests that achieved at least a 95% mass recovery were retained based on quality assurance quality control checks (Ducoste *et al.* 2001). Using the concentrations and corresponding time intervals, the retention time of each component of the disinfection system as well as the residence time density function were found using Equations (1)–(3).

$$\bar{\tau}_{\text{RTD}} = \sum_{i=0}^{i_{\text{max}}-1} \left[ \frac{E(t_i) \cdot t_i + E(t_{i+1}) \cdot t_{i+1}}{2} \right] (t_{i+1} - t_i) \quad (1)$$

$$E(t_i) = \frac{c(t_i)}{\text{area}} \quad (2)$$

$$\text{area} = \sum_{i=0}^{i_{\text{max}}-1} \left[ \frac{c(t_{i+1}) + c(t_i)}{2} \right] (t_{i+1} - t_i) \quad (3)$$

The experimental residence times computed from Equation (1) are shown in Table 1 and the RTDs for each major chamber are displayed in Figure 2.

**Table 1** | Experimental residence times for disinfection system reactors (theoretical in bold)

Flow (ml/sec)	Ozone Contactor 1 RT (sec)	Ozone Contactor 2 RT (sec)	Mixing Chamber RT (sec)	Chlorine Contactor RT (sec)
15.5	142 (156)	142 (156)	64 (65)	1901 (1992)
11	199 (220)	199 (220)	98 (91)	2705 (2807)

### Measurement of ozone Ct distribution

The Ct probability distribution function (Ct-PDF) in the ozone contactor was determined using a Markov-chain Monte Carlo (MCMC) integration of the Bayes equation. The procedure is adapted from the method applied by Bohrerova *et al.* 2005 for determining the ultraviolet (UV) dose distribution using UV sensitive fluorescence microspheres. A detailed discussion of this approach is provided in Bohrerova *et al.* (2005) and summarized here. The computed Ct-PDF was based on two parts: 1) the effluent measurements of microspheres' fluorescence from the 2nd ozone reactor and 2) the bench scale measurements of the microspheres' fluorescence intensities decay from exposure to known ozone Ct values. MCMC integration is an important step to determine the corresponding Ct distribution since a fluorescence intensity distribution was generated for each known Ct level instead of a single fluorescence value from the bench scale tests. As a result, there was some overlap in fluorescence distribution between each Ct level used in the bench scale experiments. Therefore, a single fluorescence distribution can potentially be attributed to a continuous range of corresponding Ct values.

Two separate statistical models were developed; one for the ozone contactor results and one for the bench-scale results to resolve the unknown and known fluorescence distributions, respectively. For the bench-scale experiments, the purpose was to determine the relationship between the microsphere fluorescence and Ct values. Based on Bayes' theorem, the statistical model can be described as (Bohrerova *et al.* 2005):

$$Ct_{\text{bench scale}} = \begin{cases} Fl_d \approx \text{Dist}(\mu_d, \sigma_d) \\ \mu_d = B_\mu + A_\mu Ct_d \\ \sigma_d = B_\sigma + A_\sigma Ct_d \\ Ct_d = \{Ct_{\text{bench\_scale}}\}_d \end{cases} \quad (4)$$

In Equation (4),  $Ct_{\text{bench scale}}$  is the bench scale Ct values and  $Fl_d$  is the microsphere fluorescence for a known Ct level ( $Ct_d$ ) during the bench scale experiments. Bench scale samples were exposed to Ct values of 0.18, 0.36, 0.54, 0.86, 1.23, and 1.75 mg/L-min.  $Fl_d$  can be characterized as either a normal or log normal distribution and is represented generically by  $\text{Dist}(\mu_d, \sigma_d)$ . According to Bohrerova *et al.* (2005),  $Fl_d$  was expressed as a Log-Normal distribution due to the range and shape of the microsphere fluorescence distribution when exposed to UV. These distributions were described by other researchers working with UV disinfection as Gaussians (Anderson *et al.* 2003). In the present research, a quantile-quantile (QQ) plot (also known as normal probability plot) was used to determine whether the microsphere fluorescence data follows a normal distribution. A log normal distribution was assumed if the QQ-plot did not demonstrate that the data followed a normal distribution. While the fluorescence data could follow other distributions such as Weibul, gamma, or Beta, a log-normal distribution was assumed since it is the simplest two parameter alternative whose parameters are directly based on the mean and standard deviation of the data set.

Figure 3 illustrates a QQ-plot for the microsphere fluorescence distribution from the ozone contactor operated at 11- and 15.5-ml/sec flow rate. The linear relationship between normal distribution theoretical quantiles and quantiles of the low flow experimental data suggests that the microsphere fluorescence data can be characterized by a normal distribution. However, the QQ-plot showed that a non-normal distribution was found to characterize the high flow condition. Log-normal would therefore be used for the high flow condition.

In Equation 4, a linear correlation was assumed between the averages ( $\mu$ ) and the standard deviations ( $\sigma$ ) of the fluorescence distribution for each Ct level tested in the bench scale experiments.  $B_\mu, A_\mu, B_\sigma, A_\sigma$  represent the set of fitting parameters from the bench-scale experiments statistical model.  $A_\mu$  and  $A_\sigma$  were the slopes and  $B_\mu$  and  $B_\sigma$  were the intercept of the linear fit between the Ct values and the corresponding fluorescence average and standard deviation. For both the low flow and high flow tests,  $R^2$  values greater than 0.9 were found for the linear correlation in Equation (4).

$B_\mu, A_\mu, B_\sigma$  and  $A_\sigma$  were then used as the average and standard deviation values for the ozone contactor

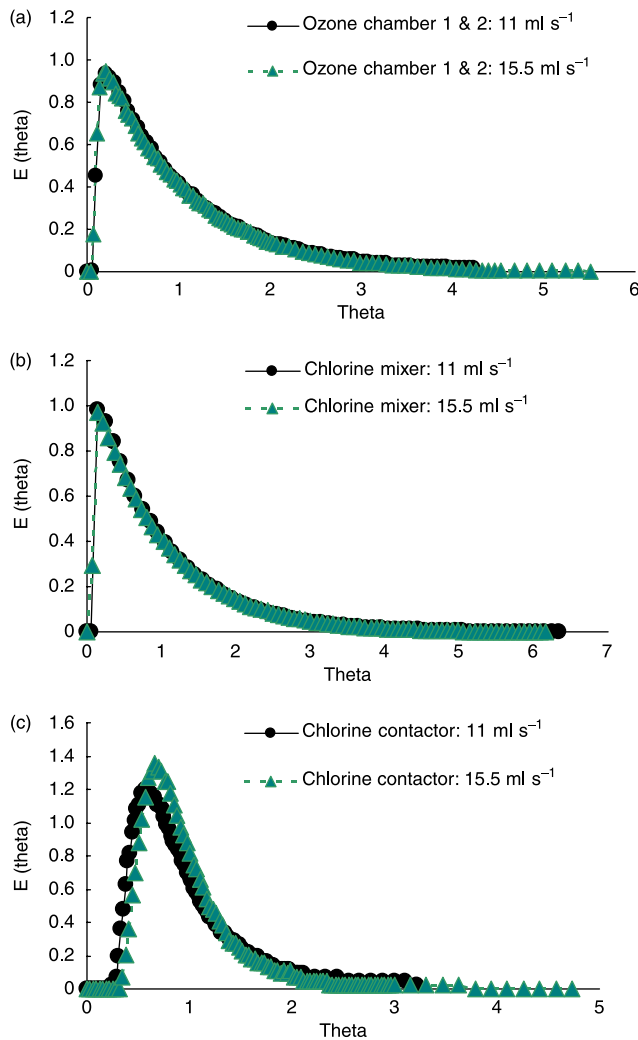


**Figure 2** | Residence time density functions for different parts of the sequential disinfection pilot system: (a) ozone chamber 1 and ozone chamber 2, (b) chlorine mixing chamber, (c) chlorine contactor.

microsphere fluorescence data. Equation (5) displays the statistical model used for the contactor fluorescence data:

$$Ct_R = \begin{cases} Fl_R \approx \text{Dist}(\mu_R, \sigma_R) \\ \mu_R = B_\mu + A_\mu Ct_R \\ \sigma_R = B_\sigma + A_\sigma Ct_R \\ Ct_R \approx \text{Gamma}(\alpha, \rho) \end{cases} \quad (5)$$

The  $Ct$  distribution in the ozone contactor ( $Ct_R$ ) was assumed to take the shape of a Gamma distribution since it can produce a broad range of shapes that includes log-normal and

Weibull distributions. For the Gamma distribution, the shape parameter ( $\alpha$ ) and rate parameter ( $\rho$ ) were assumed prior Pareto distribution (with  $c_1 = 1$  and  $c_2 = 8$ ) that defines a decreasing distribution between  $c_2$  and  $\infty$  and exponential distribution (with  $\lambda_2 = 0.0001$ ), respectively (Equation (6)). Exponential prior distributions were assigned to  $B_\mu$ ,  $A_\mu$ ,  $B_\sigma$  and  $A_\sigma$  with a decay rate of  $\lambda_2$ , that defines it as a slowly decaying distribution between 0 and  $\infty$ .

$$\begin{cases} \alpha \\ \rho \end{cases} = \begin{cases} \text{Pareto}(c_1, c_2) \\ \text{Exp}(\lambda_2) \end{cases} \quad (6)$$

As in Bohrerova *et al.* (2005), a range of  $c_2$  values were tested to explore its sensitivity to the results and no difference was found beyond a value of 8. “R.2.5.0” statistical software was used to generate the best estimate for  $B_\mu$ ,  $A_\mu$ ,  $B_\sigma$ ,  $A_\sigma$  and the initial data input for WINBUGS 1.4, that was used to generate the best estimates for  $\alpha$  and  $\rho$  using MCMC integration. 1000 pairs of  $\alpha$  and  $\rho$ , generated by WINBUGS, were re-sampled by “R.2.5.0” to generate the ozone contactor  $Ct$  distribution.

### Disinfection system model

The inactivation of *Cryptosporidium* in the continuous-flow disinfection system was evaluated using the Segregated Flow Reactor (SFR) model. Microbial inactivation based on the SFR approach was calculated using the residence time density function in the following equation:

$$N/N_0 \text{ Effluent} = \int_0^{T \text{ max}} [(N/N_0)(t)]_{\text{bench}} * E(t) dt \quad (7)$$

$[(N/N_0)(t)]_{\text{bench}}$  is the bench-scale survival rate at time  $t$  and  $E(t)$  is the experimental RTD.

In this study, the Chick-Watson (CW) model (Equation (8)) was used to describe the inactivation kinetics during ozone primary treatment and chlorine treatment when it was used without ozone. A disinfectant decay term was not needed in the CW model since experimental measurements of the disinfectant displayed no change between the influent and effluent location. During sequential disinfection, a two component CW model (Equation (9)) was used to capture the two sloped curve observed by Driedger *et al.* (2000).

$$[N/N_0(t)]_{\text{bench}} = \exp(-k_{cw} Ct) \quad (8)$$

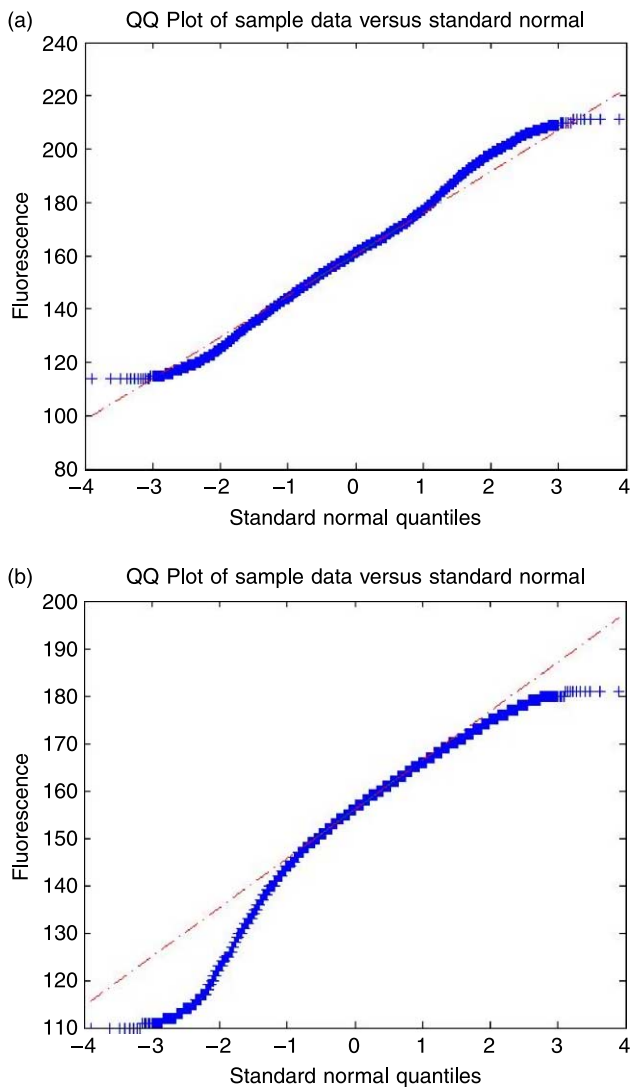


**Figure 3** | QQ-plot for microsphere fluorescence distribution data from the ozone contactor experiments: (a) Low flow, (b) High flow.

$$[N/N_0(t)]_{\text{bench}} = (1 - f) \exp(-k_1 Ct) + f \exp(-k_2 Ct) \quad (9)$$

In Equations (8) and (9),  $k_{\text{CW}}$  represents the CW inactivation rate constant,  $k_1$  and  $k_2$  are the two rate constants in the two component CW model,  $C$  is the disinfectant concentration,  $N$  is the number of live microorganisms,  $t$  is the contact time, and  $f$  is the fraction of microorganisms following an inactivation rate constant equal to  $k_2$ . The constants for both ozone and chlorine inactivation were determined from Driedger *et al.* (2000)

and were defined as follows:  $k_{\text{CW}}(\text{ozone}) = 1.5 \text{ L/mg-min}$ ,  $k_{\text{CW}}(\text{chlorine, non-sequential}) = 0.0015 \text{ L/mg-min}$ ,  $k_1 = 0.008 \text{ L/mg-min}$ ,  $k_2 = 0.003 \text{ L/mg-min}$ ,  $f = 0.054$ .

The SFR model assumes that each fluid parcel behaves as a completely mixed batch reactor that remains completely segregated (i.e., not mixed) with other fluid parcels. The SFR was used in this study to determine if a simple modeling approach could characterize the sequential disinfection process. Equation (7) will be used to compute the effluent log inactivation at three locations in the disinfection system; following the 2nd ozone contactor, mixing chamber, and the baffled chlorine contactor.

## RESULTS AND DISCUSSION

### Microspheres pretreatment and threshold determination

The microspheres used in this research had an initial fluorescence intensity that was greater than the fluorescence intensity needed to imitate the *Cryptosporidium* inactivation reference data. Therefore, the microspheres were pretreated so that the initial fluorescence intensity could be reduced. The fluorescence threshold value was used to calibrate the microspheres' fluorescence decay to the *Cryptosporidium* inactivation data of Driedger *et al.* (2000).

The threshold value was found by using the least squares method. This threshold value was used for the remainder of the experiments performed with a particular batch of pretreated microspheres. Figure 4 displays an example of a batch test following ozone pretreatment and shows how only one threshold value ( $\text{Th} = 65$ , in this case) can accurately imitate the *Cryptosporidium* inactivation kinetics reference data.

### Primary disinfection with ozone

Ozone disinfection experiments were conducted at  $\text{pH} = 7.5$  and temperature =  $20 \pm 2^\circ\text{C}$ . Primary ozone disinfection experiments were performed after ozone pretreatment. The results showed that a microsphere fluorescence decay of approximately one-log was achieved during primary ozone treatment with log reduction values

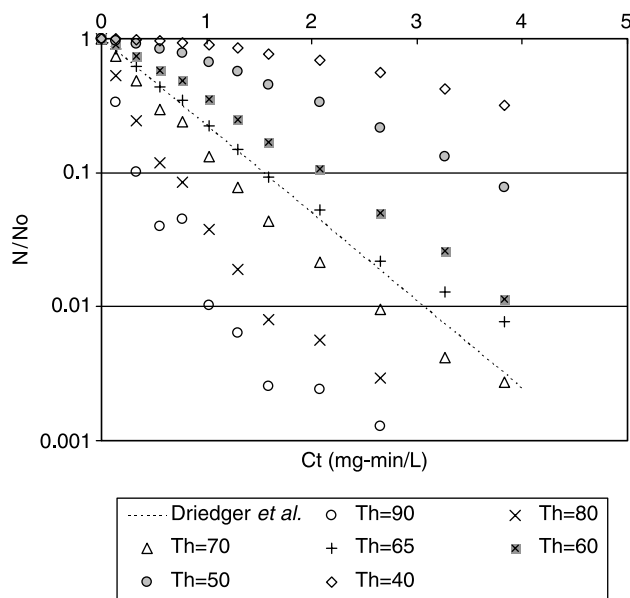


**Figure 4** | Microspheres inactivation with ozone (0.29 mg/L) at pH 7.5,  $20 \pm 2^\circ\text{C}$ , and for a duration of 90 min. Reference inactivation curve based on Driedger *et al.* (2000).

between 0.81 to 0.88 for the low flow rate and 0.71–0.8 for the high flow rate conditions. The flow rate and ozone concentration in the two column ozonators was designed to achieve approximately one-log reduction to imitate the primary ozone treatment of *Cryptosporidium* from Driedger *et al.* (2000).

### Chlorine disinfection

Table 2 displays the results of sequential and non-sequential free chlorine disinfection experiments. Sampling locations are shown in Figure 1. In Table 2, the microspheres exposed to chlorine without any ozone primary treatment displayed a similar reduction in fluorescence between the different measurement locations (i.e., the drop between the chlorine injection point in the mixing chamber and location 1 in the chlorine contactor is similar to the drop between locations 1 and 2 and between locations 2 and 3). The effluent log reduction when only chlorine was applied was less than one. However, when chlorine was applied after ozone primary treatment, the microspheres, like the *Cryptosporidium* reference data (Driedger *et al.* 2000), showed an improved log reduction, achieving almost two log reduction in the chlorine contactor effluent (Location 3). The data in

Table 2 showed that a significant portion of that effluent log reduction occurred between the chlorine injection point and location 1.

The initial ozone exposure broke down outer layers of the microsphere, exposing dye on the inner layers. The chlorine reacted quickly with the exposed dye causing a higher initial fluorescence decay and then slowly penetrated the remaining layers and reacted with the dye in those layers. The results of a previous study showed that ozone is able to erode the polymer matrix, allowing the free chlorine to readily react with the dye available on the layers now exposed after ozone treatment (Baeza & Ducoste 2004). When compared to the chlorine-only disinfection tests, the results with ozone followed by chlorine demonstrated the ability of the fluorescence microspheres to mimic synergistic effects in the continuous flow system.

### Simulated microbial inactivation

The microspheres fluorescence decay was modeled using the Chick-Watson model when ozone was used for the primary disinfectant and when analyzing the disinfection performance of chlorine non-sequentially (Equation (7)). A two-component Chick-Watson model was used to describe the fluorescence decay kinetics for chlorine when used as the secondary disinfectant after primary ozone disinfection treatment. The log reduction results given by the SFR model for the continuous flow disinfection process are shown in Table 3.

The results in Table 3 show that following ozone disinfection (i.e., in the effluent of ozone chamber 2), the SFR model significantly over-predicts the experimental log reduction for the high flow condition and slightly over-predicts the experimental log reduction for the low flow conditions. When compared to the experimental effluent results of the chlorine contactor, the model significantly over-predicted the log reduction for both flow rate conditions. The overall experimental log fluorescence removal for the sequential disinfection system was 1.9 and 1.6 for the 11- and 15.5-ml/s flow conditions, respectively, while the model predicted 2.4 and 2.5 for the 11- and 15.5-ml/s flow conditions, respectively. The SFR approach was able to show the higher log reduction when applying two sequential disinfectants compared to chlorine alone.

**Table 2** | Chlorine primary and secondary disinfection tests (measurement in chlorine contactor)

<b>Chlorine sequential disinfection</b>						
Experiment	LF-1	LF-2	LF-3	HF-1	HF-2	HF-3
Flow (ml/sec)		11.0			15.5	
Chlorine concentration (mg/L)	12.8	12.2	13.1	15.8	16.4	17.1
–Log(N/No) location 1	1.30	1.33	1.38	1.16	1.19	1.16
–Log(N/No) location 2	1.44	1.48	1.55	1.39	1.41	1.39
–Log(N/No) location 3	1.89	1.77	2.05	1.47	1.68	1.50
<b>Chlorine non-sequential disinfection</b>						
Experiment	LF-1	LF-2	LF-3	HF-1	HF-2	HF-3
Chlorine concentration (mg/L)	12.8	12.2	13.1	16.2	16.8	17.4
–Log(N/No) location 1	0.10	0.10	0.11	0.12	0.13	0.12
–Log(N/No) location 2	0.32	0.23	0.29	0.23	0.27	0.22
–Log(N/No) location 3	0.68	0.61	0.63	0.48	0.55	0.51

However, for the non-sequential conditions, the SFR model predicted a lower effluent log reduction than the experimental results regardless of the flow rate. In addition to these discrepancies, the model did not consistently capture the correct trend in the experimental log reduction data between the 11- and 15-ml/s flow conditions.

One contribution to the model discrepancy is due to the higher secondary disinfectant rate kinetics for *Cryptosporidium* from Driedger *et al.* (2000) than the actual fluorescent dye decay rate kinetics in the microspheres. In the study performed by Baeza & Ducoste (2004), the secondary disinfectant fluorescent dye decay kinetics was found to be slightly slower than the *Cryptosporidium*

secondary disinfectant inactivation kinetics (*Cryptosporidium* kinetics = 0.008, 0.003; microspheres kinetics = 0.007, 0.003). For the non-sequential chlorine tests, the *Cryptosporidium* inactivation kinetics was lower compared to the microspheres dye decay kinetics found in this study (*Cryptosporidium* kinetics = 0.0015; microspheres kinetics ≈ 0.003). However, this is only a small contribution to the error and would not completely explain the difference found between the model predictions and the experimental results.

Another possible reason for the model discrepancy could be due to the segregated mixing assumption of the SFR approach. As discussed earlier, the SFR model assumes

**Table 3** | Comparison between experimental and numerical Log reduction

	–Log(N/No) for low flow conditions		–Log(N/No) for high flow conditions	
	Experimental with 95% CI in bold	SFR	Experimental with 95% CI in bold	SFR
<b>Sequential disinfection</b>				
Ozone 1	–	–	–	–
Ozone 2	0.84 (0.80–0.89)	0.87	0.76 (0.71–0.85)	1.02
Chlorine location 1	1.34 (1.30–1.38)	–	1.21 (1.13–1.32)	–
Chlorine location 2	1.48 (1.43–1.55)	–	1.42 (1.38–1.48)	–
Chlorine location 3	1.89 (1.77–2.05)	2.40	1.55 (1.44–1.70)	2.52
<b>Non-sequential disinfection</b>				
Chlorine location 1	0.10 (0.10–0.11)	–	0.12 (0.11–0.13)	–
Chlorine location 2	0.28 (0.23–0.33)	–	0.24 (0.21–0.27)	–
Chlorine location 3	0.63 (0.60–0.68)	0.34	0.51 (0.47–0.56)	0.32

that each parcel of fluid is a completely mixed batch reactor whose water molecules remain independent of other fluid parcels. This is not completely the case for continuous flow systems that have a high degree of spatial variations in turbulent energy dissipation rates or large reactor mean residence times.

When the local turbulent energy dissipation rate is high, adjacent fluid parcels will not remain grouped or unmixed with other fluid parcels. This local exchange between fluid parcels would adjust the extent of reaction due to a change in local reactant concentration. This same exchange between adjacent parcels would also occur even at small local energy dissipation rates albeit much more slowly and consequently with little impact on the SFR model if the mean residence time is small. However, for reactors with long mean residence times, mixing between adjacent fluid parcels may occur that could lead to a similar change in the extent of reaction from a local change in the reactant concentration. As mentioned earlier, the secondary chlorine reaction kinetics is nonlinear with two components: an initial fast decay followed by a slower decay range (Equation (9)). When nonlinear kinetics are utilized with the SFR approach, the extent of adjacent fluid parcel mixing can result in a larger deviation between the SFR prediction and the actual reaction conversion with increasing reaction order rates.

One could argue that the SFR model is fine and that if the model parameters (rate constants,  $k_{cw}$ ,  $k_1$ ,  $k_2$  and population fraction,  $f$ ) were calibrated at one operating condition, then it may be able to predict all other operating conditions. Table 4 displays the predicted log reduction results of the SFR model given model parameters calibrated by either the low or high flow conditions. In Table 4, the SFR model for sequential disinfection still displayed significant differences (i.e., approximately 17%) in predicting the low flow condition when calibrating the model with the high flow condition. Slightly lower percent error was found when the SFR model was calibrated with the low flow condition to predict the high flow condition (i.e., 15 and 9% for the ozone effluent and chlorine effluent, respectively). Better predictions were also found when performing this calibration procedure for the non-sequential conditions (i.e., less than 7% difference). When the calibration procedure involved either the low flow or high flow data, the percent error was clearly smaller than those produced when using the literature values. The use of literature values produced errors greater than 27% in all cases except for ozone effluent at the low flow condition, that displayed a 3% error. In addition, the direction of the change in log reduction between the low flow and high flow conditions was correct in every case with this alternative model calibration approach. This proper change in log reduction was not consistently found when using the

**Table 4** | SFR model parameter analysis

Model parameters	Literature		Optimized fit low flow		Optimized fit high flow	
<b>Sequential disinfection</b>						
$k_{cw}$	1.500		1.443		1.004	
$K_1$	0.008		0.0065		0.0038	
$K_2$	0.003		0.00073		0.0027	
F	0.052		0.054		0.043	
<b>Non-sequential disinfection</b>						
$k_{cw}$	0.0015		0.003		0.0025	
Location	Low flow	High flow	Low flow	High flow	Low flow	High flow
<b>Sequential disinfection</b>						
	– log(N/No)		– log(N/No)		– log(N/No)	
Ozone effluent	0.87	1.02	0.84	0.64	0.99	0.76
Chlorine effluent	2.40	2.52	1.89	1.41	2.22	1.55
<b>Non-sequential disinfection</b>						
Chlorine effluent	0.34	0.32	0.63	0.55	0.60	0.51

literature values for the model parameters. The results in Table 4 suggest that while the SFR sequential disinfection model when calibrated using the pilot data does yield dramatically better predictions of the process log reduction, a significant error still remains. The discrepancy between the model and experimental results may be due to the usage of a single fluorescence decay rate kinetics for the secondary chlorine disinfectant after a primary application of ozone.

The chlorine sequential fluorescence decay kinetics was based on a single Ct of 1.4 mg/L-min from Driedger *et al.* (2000). However, in this continuous flow system, each microorganism may spend a different amount of time within the ozone contactors, thus experiencing a range of primary disinfectant Ct values. Different Ct values may lead to different fluorescence decay or different *Cryptosporidium* inactivation kinetics for the secondary chlorine disinfectant since synergistic effects have been revealed in this research as well as in the literature (Driedger *et al.* 2000; Baeza & Ducoste 2004). The microspheres' data were used to generate a Ct distribution described earlier and are presented in Figure 5.

In Figure 5, the average Ct from the distributions does indicate that the target Ct was met but a distribution of Ct values does exist. The low flow Ct distribution is much broader (i.e., higher coefficient of variation) than the high flow condition. The change in the Ct distribution shape indicates subtle changes in the travel paths of the microspheres moving from the first ozone column that had a lower average ozone concentration into the second ozone column with a higher average ozone concentration. The distributions

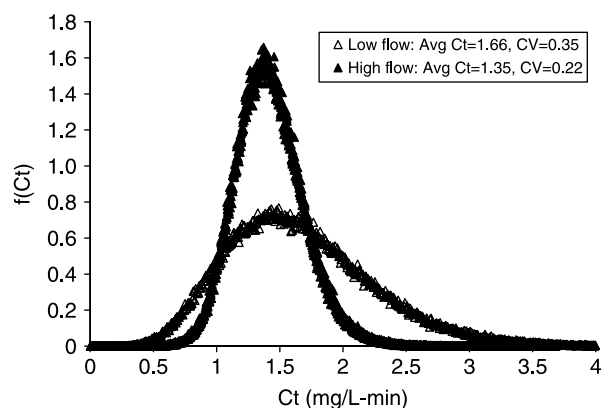


Figure 5 | Ozone effluent Ct distribution.

in Figure 5 seem to confirm the complexity in evaluating a single secondary disinfectant kinetics based on initial exposure to one primary disinfectant Ct value. In addition, the change in the coefficient of variation between the low and high flow conditions may help to explain why there was a larger error associated with calibrating the SFR model with high flow experimental results to predict the low flow results. The range of ozone Cts for the low flow condition was 0.5 to 3.2 mg/L-min and 0.8 to 2.2 mg/l-min for the high flow condition. Therefore, in order predict the level of sequential disinfection achieved by the secondary disinfectant, a clear evaluation of the variation in the secondary disinfection kinetics must be performed from a range of exposure to primary disinfectant Cts. Unfortunately, the incorporation of multiple secondary disinfectant inactivation kinetics into a numerical model may not be a simple task since the model would have to account for the cumulative primary disinfectant Ct dose received by each microorganism prior to exposure to the secondary disinfectant.

An alternative approach that could be used to simulate this kind of complex sequential disinfection interaction is by modeling the hydrodynamics, disinfectant and microbial transport using computational fluid dynamics (CFD). The proposed modeling approach could be divided into three parts: 1) simulation of the fluid mechanics with an Eulerian description of the ozone and chlorine transport and disinfectant reaction kinetics, 2) a Lagrangian description of the microbial transport through particle tracks, and 3) coordination of the particle tracks to determine the ozone Ct dose, chlorine Ct dose, and subsequent sequential log inactivation.

In part one, the velocity and turbulence within the ozone chambers would be performed using a two phase model to capture the gas dynamics on the liquid flow pattern along with the ozone mass transfer between the gas and liquid phase. A single phase approach can be used to model the chlorine transport and any remaining liquid phase ozone in the chlorine mixing chamber and the chlorine contactor. The liquid phase ozone concentration and chlorine concentration would be modeled as a chemically reacting tracer (i.e., Eulerian framework). In part two, the particle trajectory can be determined by solving either the particle momentum equation or by utilizing a random-walk algorithm. At each time step, the value for the ozone concentration and chlorine

concentration would be recorded. The cumulative ozone Ct dose and chlorine Ct dose would be determined as follows:

$$\text{Dose}_{\text{disinfectant}} = \int_0^{\infty} C_{\text{disinfectant}} dt \quad (10)$$

The calculation described in Equation (10) would be performed for each particle track released at the influent of the sequential disinfection system. Once the ozone Ct dose is computed for each particle track, the log inactivation for ozone disinfection can be computed. In addition, knowledge of the cumulative ozone Ct dose for that particular particle track allows the determination of the appropriate secondary inactivation kinetics that should be used with the cumulative chlorine dose. The proposed modeling approach described above is only one approach and others may exist. However, the proposed model does provide a framework to explore the simulation of sequential disinfection processes where synergistic behavior has been noted between the two or more disinfectants.

## CONCLUSION

Experimental research was conducted to demonstrate the use of YG Fluoresbrite™ microspheres as a non-biological surrogate for *Cryptosporidium* disinfection under sequential disinfection conditions in a continuous flow water treatment system. Tests were performed at two flow rates in a system that consisted of ozone as a primary disinfectant followed by chlorine as a secondary disinfectant. Experimental analysis of the microspheres fluorescence decay using two disinfectants demonstrated that the YG microsphere could imitate enhanced secondary disinfectant performance and mimic the behavior of *Cryptosporidium* sequential disinfection in a continuous flow disinfection system.

A simple Segregated Flow Reactor (SFR) model was used to simulate the microspheres' fluorescence decay process given the sequential *Cryptosporidium* inactivation kinetics from the literature and the residence time distribution. Overall, the model was able to demonstrate the enhanced log reduction when chlorine was applied following ozone primary treatment. However, the SFR approach

fell short of predicting sequential secondary enhanced chlorine fluorescence decay observed by the microspheres when calibrated using literature *Cryptosporidium* inactivation kinetics. Major contributions to the discrepancies between the SFR model and microsphere experimental results include the segregated mixing assumptions of the SFR model and the change in secondary disinfection kinetics due to the distribution of primary disinfectant Ct values. Improvements to the SFR model predictions were found when the model was calibrated using either the low or high flow data. However, analysis of the fluorescence microspheres from the effluent of the ozone system confirmed the existence of a Ct distribution and that a wider distribution was found at the low flow condition compared to the high flow condition. The existence of a Ct distribution impacted the SFR model performance.

A proposed alternative model was described that involves the use of CFD to simulate the sequential disinfection process. The proposed model would simulate the disinfectants transport and reaction in an Eulerian framework and model the transport of microorganisms in a Lagrangian particle tracking framework. These particle tracks would then be used to compute the primary disinfectant dose so that the appropriate secondary disinfection kinetics could be used to determine the final log reduction of the sequential disinfection system.

## ACKNOWLEDGEMENTS

This research was sponsored in part by the National Science Foundation (NSF) through NSF- BES-0092647 and the Water Resources and Environmental Engineering program, Department of Civil, Construction, and Environmental Engineering, NCSU.

## REFERENCES

- Anderson, W. A., Zhang, L., Andrews, S. A. & Bolton, J. R. 2003 A technique for direct measurement of UV fluence distribution In: *Proceedings of the Water Quality Technology Conference 2003*. American Water Works Association, Philadelphia, PA. AWWA, Denver, CO. CD Rom.

- Baeza, C. A. & Ducoste, J. J. 2004 A non-biological surrogate for sequential disinfection processes. *Water Res.* **38**(14–15), 3400–3410.
- Bohrerova, Z., Bohrer, G., Mohanraj, S., Ducoste, J. & Linden, K. G. 2005 Experimental measurements of fluence distribution in a UV reactor using fluorescent dyed microspheres. *Environ. Sci. Technol.* **39**, 8925–8930.
- Chiou, C. F., TorresLugo, M., Mariñas, B. J. & Adams, J. Q. 1997 Nonbiological surrogate indicators for assessing ozone disinfection. *J. Am. Water Works Assoc.* **89**(8), 54–66.
- Corona-Vasquez, B., Rennecker, J. L., Driedger, A. M. & Mariñas, B. J. 2002a Sequential inactivation of *Cryptosporidium parvum* oocysts with chlorine dioxide followed by free chlorine or monochloramine. *Water Res.* **36**(1), 178–188.
- Corona-Vasquez, B., Samuelson, A., Rennecker, J. L. & Mariñas, B. J. 2002b Inactivation of *Cryptosporidium parvum* oocysts with ozone and free chlorine. *Water Res.* **36**(16), 4053–4063.
- Driedger, A. M., Rennecker, J. L. & Mariñas, B. J. 2000 Sequential inactivation of *Cryptosporidium parvum* oocysts with ozone and free chlorine. *Water Res.* **34**(14), 3591–3597.
- Ducoste, J., Carlson, K. & Bellamy, W. 2001 The integrated disinfection design framework approach to reactor hydraulics. *J. Water Supply: Res. Technol.* **50**(4), 245–261.
- Greene, D. J., Farouk, B. & Haas, C. N. 2004 CFD design approach for chlorine disinfection processes. *AWWA J.* **96**(8), 138–150.
- Gyurek, L. L., Finch, G. R. & Belosevic, M. 1997 Modeling chlorine inactivation requirements of *Cryptosporidium parvum* oocysts. *J. Environ. Eng.-ASCE* **123**(9), 865–875.
- Haas, C. N., Joffe, J., Heath, M., Jacangelo, J. & Anmangandla, U. 1998 Predicting disinfection performance in continuous flow systems from batch disinfection kinetics. *Water Sci. Technol.* **38**(6), 171–179.
- Kim, J. H., Corona-Vasquez, B. & Mariñas, B. 2002 Mechanistic approach for modeling the inactivation of microbial contaminants with chemical disinfectants. *American Water Works Association Water Quality and Technology Conference*. AWWA, Denver, CO.
- Larson, M. A. & Mariñas, B. J. 2003 Inactivation of *Bacillus subtilis* spores with ozone and monochloramine. *Water Res.* **37**(4), 833–844.
- Li, H., Finch, G. R. & Smith, D. W. 2001a Sequential Disinfection Design Criteria for Inactivation of *Cryptosporidium* Oocysts in Drinking Water. AWWA Research Foundation & The American Water Works Association, Denver, CO, USA.
- Li, H., Finch, G. R., Smith, D. W. & Belosevic, M. 2001b Sequential inactivation of *Cryptosporidium parvum* using ozone and chlorine. *Water Res.* **35**(18), 4339–4348.
- Liyanage, L. R. J., Finch, G. R. & Belosevic, M. 1997 Sequential disinfection of *Cryptosporidium Parvum* by ozone and chlorine dioxide. *Ozone Sci. Eng.* **19**, 409–423.
- Mariñas, B. J., Rennecker, J. L., Hung, C., Teefy, S., Rice, E. W. & Owens, J. H. 1997 Assessment of ozone disinfection efficiency using fluorescent-dyed polystyrene microspheres as indicators for *Cryptosporidium* oocysts. *American Water Works Association, Annual Conference Proceedings*, Atlanta-GA. AWWA, Denver, CO. pp. 531–544.
- Mariñas, B. J., Rennecker, J. L., Teefy, S. & Rice, E. W. 1999 Assessing ozone disinfection with nonbiological surrogates. *J. Am. Water Works Assoc.* **91**(9), 79–89.
- Rennecker, J. L., Corona-Vasquez, B., Driedger, A. M. & Mariñas, B. J. 2000a Synergism in sequential disinfection of *Cryptosporidium parvum*. *Water Sci. Technol.* **41**(7), 47–52.
- Rennecker, J. L., Driedger, A. M., Rubin, S. A. & Mariñas, B. J. 2000b Synergy in sequential inactivation of *Cryptosporidium parvum* with ozone/free chlorine and ozone/monochloramine. *Water Res.* **34**(17), 4121–4130.
- Rennecker, J. L., Corona-Vasquez, B., Driedger, A. M., Rubin, S. A. & Mariñas, B. J. 2001 Inactivation of *Cryptosporidium parvum* oocysts with sequential application of ozone and combined chlorine. *Water Sci. Technol.* **43**(12), 167–170.
- Trotter, J. 2000 *WinMDI Version 2.8 – (Windows Multiple Document Interface for Flow Cytometry)*. Scripps Institute. <http://facs.scripps.edu/software.html>
- Vasconcelos, J. J., Rossman, L. A., Grayman, W. M., Boulos, P. F. & Clark, R. M. 1997 Kinetics of chlorine decay. *J. Am. Water Works Assoc.* **89**(7), 54–65.
- US Environmental Protection Agency 1998 National primary drinking water regulations: interim enhanced surface water treatment; final rule. *Fed. Regul.* **63**(241), 69478.
- US Environmental Protection Agency 2002 National primary drinking water regulations: long term 1 enhanced surface water treatment rule; final rule. *Fed. Regul.* **67**(9), 1812.

First received 11 July 2007; accepted in revised form 2 October 2007